

## STUDY OF $\text{Cu}_2\text{ZnSnSe}_4$ THIN FILMS PREPARED BY E-BEAM EVAPORATION OF SOLID-STATE REACTED COMPOUND

R. PRAJAPAT\*, Y. C. SHARMA

Department of Physics, Vivekananda Global University, Jaipur-303012, Rajasthan

A quaternary semiconductor  $\text{Cu}_2\text{ZnSnSe}_4$  (CZTSe) has been emerged as a paramount candidate in form of absorber layer in thin film solar cell. CZTSe holds additional advantages like non-toxic constituents, abundant in earth crust and low cost over other chalcogenides like CIGS, CdTe etc. In this paper we have reported the growth of CZTSe thin films using pre-synthesized bulk CZTSe solid state reacted compound as a source in e-beam evaporation deposition technique. Firstly bulk CZTSe compound in five different ratios were prepared using elemental constituents of Cu, Zn, Sn and Se. These five solid state reacted compounds were used as a target for thin film deposition. The Cu/(Zn+Sn) ratio in these films vary nearly to stoichiometry. The structural result analysis carried out using XRD data of thin films confirmed that phase content was noticeably affected during the film deposition process with respect to Cu/(Zn+Sn) ratios variation. Some amount of secondary phases were also found in the samples. Compositional variation in elemental constituents was studied by SEM-EDX and mapping spectra.

(Received: August 1, 2019; Accepted November 28, 2019)

*Keywords:* Thin films, XRD, SEM

### 1. Introduction

A serious consideration is increased towards the renewable energy resources due to increasing energy demand over to fossil fuel sources. Photovoltaic technology has been extensively emerged with latest innovations in recent years to develop and increase the efficiency of thin film solar cell. Kesterite semiconductors like  $\text{Cu}_2\text{ZnSnSe}_4$  and  $\text{Cu}_2\text{ZnSnS}_4$  are commercially developed as an absorber layer in thin film solar cell based on some special properties like earth abundant material and non-toxicity. The earlier investigations shows that CZTSe have been deposited by spray pyrolysis method and corresponding solar cell showed conversion efficiency of 2.39%. [1] Lots of deposition techniques have been employed by many researchers to fabricate CZTSe thin films like spray pyrolysis, thermal evaporation etc. [1] XRD studies reveals that thermally evaporated CZTSe thin films exhibited the Kesterite structure with unit cell dimension  $a = 0.569\text{nm}$  and  $c = 1.139\text{nm}$  with band gap lying within the range of 1.0 eV and 1.4 eV. [2]

A deep investigations have been done using in situ laser light scattering and ex situ characterization techniques for CZTSe as some other detrimental phases like ZnSe and  $\text{Cu}_{2-x}\text{Se}$  developed during the deposition process highly influences the solar cell device performance. [3] Septina et al. in their study showed that annealing of electrodeposited CZTSe under Ar gas flow caused losses of Sn and Se precursors due to evaporation of SnSe and device showed the conversion efficiency of 1.1%. [4] Khalil et al. successfully fabricated CZTSe solar cell approaching the electrochemical method for the synthesis of CZTSe with conversion efficiency of 0.1%. [5] Lex et al reported the controlled selenization of thermally evaporated CZT structure to fabricate CZTSe from industrialization point of view at  $450^\circ\text{C}$  and concluded that the value of absorption coefficient of  $104\text{cm}^{-1}$  with resistivity of  $30\ \Omega\cdot\text{cm}$  was exhibited by CZTSe in conjunction with the band gap of 1.52 eV. [6] To investigate the influence of stoichiometry variations in CZTSe, Chinnaiyah and his coworkers successfully prepared

---

\* Corresponding author: rekhaprajapat7@gmail.com

$\text{Cu}_2\text{Zn}_{1.5}\text{Sn}_{1.2}\text{Se}_{4+x}$  alloys and presented an overview that pure CZTSe phase was obtained for the value of  $x=0.8$  with p-type conduction.[7]

Characterization of polycrystalline CZTSe thin films discloses that selenization process of CZTSe between the temperature range of 480°C-540°C showed Kesterite structure having orientation along (112) direction with optical band gap ranging from 0.88 to 0.93 eV due to loss of  $\text{SnSe}_x$  phase and solar cell designed from CZTSe selenized at 500°C showed the fill factor and conversion efficiency of 44 % and 7.18% respectively.[8] Furthermore photoluminescence study of selenized sputtered CZTSe reveals that intense and narrow band was resolved by high quality films showing two photon replica.[9] The results confirm that the annealing temperature is a dominating reason for the formation of detrimental phases during the annealing process. It is also desirable to control the formation of phases as selenization of CZT layers at 250°C lead to formation of phase  $\text{Cu}_6\text{Sn}_5$  .[10]

## 2. Experimental

CZTSe thin films have been grown by employing two stage process: (i) In first step bulk CZTSe has been synthesized using Cu, Zn, Sn and Se powders (99.99% pure) by solid state reaction method. CZTSe is prepared with varying the Cu/(Zn+Sn) ratio in number of five samples. The elemental precursors were weighed in the five different molar ratios with chemical composition as presented in table 1. These weighed elements were sealed in quartz ampoule at a pressure of  $1 \times 10^{-6}$  Torr and were allowed to heat up in furnace for 3 hours. After the cooling process chunks were separated from the ampoules and were grinded into square shape.

(ii) Prior to the film deposition from pre-synthesized bulk CZTSe, substrates (Soda lime glass) were ultrasonically cleaned in acetone and hot bath were given at the temperature of 70° C with 60 rpm. Cleaned and dried substrates were mounted on the substrate holder to place in the E-Beam deposition unit. Substrates were rotated at constant rate for uniform deposition and were put up in the line of sight of the crucible. The supply voltage of 5.20KV with current of 1 mA was applied for deposition and the deposition chamber was evacuated to the vacuum of  $1.5 \times 10^{-5}$  mbar.

Five samples of CZTSe thin films were prepared with variation in Cu/(Zn+Sn) ratio with different stoichiometry as mentioned in table 1 below. XRD measurements have been performed to study the structural features of synthesized and deposited thin films. SEM-EDX of the thin films was done to confirm the stoichiometry variation.

Table 1. Stoichiometry variations in ratio of solid state reacted CZTSe compound.

Sample	Stoichiometry	Cu/Zn	Cu/Sn	Se/(Cu+Zn+Sn)	Cu/(Zn+Sn)
Sample 1	$\text{Cu}_2\text{ZnSnSe}_4$	2.0	2.0	1.0	1.0
Sample 2	$\text{Cu}_2\text{ZnSnSe}_{5.6}$	2.0	2.0	1.4	1.0
Sample 3	$\text{Cu}_2\text{ZnSnSe}_{5.2}$	2.0	2.0	1.3	1.0
Sample 4	$\text{Cu}_{1.8}\text{ZnSnSe}_{5.2}$	1.8	1.8	1.36	0.9
Sample 5	$\text{Cu}_2\text{Zn}_{1.1}\text{SnSe}_{5.2}$	1.818	2.0	1.26	0.95

## 3. Results

### 3.1 CZTSe bulk

#### 3.1.1. Structure and phase analysis

Study of Structural features of synthesized bulk CZTSe material is done by XRD. Figure 1 shows the XRD spectra recorded for CZTSe (bulk) prepared by employing the conventional method of solid state reaction method. Analytical report of CZTSe bulk confirms the formation of CZTSe phase with some secondary phases. It could be easily seen from the pattern that the dominating peak located at 38.82° corresponds to  $\text{Cu}_2\text{ZnSnSe}_4$ . [11] An additional peak at the value of  $2\theta=23.21^\circ$  attributes to  $\text{Cu}_2\text{SnSe}_3$  phase.[12]

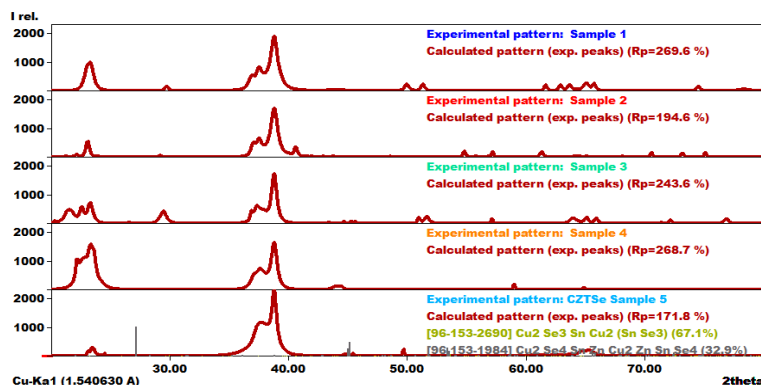


Fig. 1. XRD pattern for bulk CZTSe compound synthesized by solid state reaction.

The crystallite size is calculated by using Scherrer's formula given below

$$D = \frac{0.9\lambda}{\beta \cos\theta}$$

where  $\lambda$  is the wavelength of the radiation used in XRD characterization, D is crystallite size and  $\beta$  is FWHM in radians for the most intense peak. The crystallite size is found 21.6 nm for bulk CZTSe samples.

CZTSe with space group I-42 m (121) is exhibiting tetragonal crystal structure with unit cell parameters  $a = 5.68820 \text{ \AA}$   $c = 11.33780 \text{ \AA}$  with Wyckoff parameters listed in table 2 below:

Table 2. Structural parameters of Sample 1.

Empirical formula	Crystal system	Space group	Unit Cell dimension ( $\text{\AA}$ )	$I/I_c$	$c/2a$	Density (calculated) $\text{gm/cm}^3$	Wyckoff position			
							X	Y	Z	
$\text{Cu}_2\text{ZnSnSe}_4$	Tetragonal	I -4 2 m (121)	$a = 5.68820$ $c = 11.33780$	13.17	0.9959	5.6760	Sn	0.000	0.000	0.500
							Se	0.259	0.259	0.371
							Cu	0.000	0.500	0.250
							Zn	0.000	0.000	0.000
$\text{Cu}_2\text{SnSe}_3$	Monoclinic	C 1 c 1 (9)	$a = 6.96700$ $b = 12.04930$ $c = 6.94530$ $\beta = 109.190^\circ$	6.450	0.4989	5.82200	Cu	0.370	0.418	0.116
							Cu	0.371	0.257	0.616
							Sn	0.363	0.091	0.107
							Se	0.503	0.259	-0.014
							Se	-0.026	0.078	-0.015
Se	0.00	0.409	0.000							

### 3.2. CZTSe thin films

#### 3.2.1. Structural and phase analysis

Thin films prepared in five different elemental ratios from the e-beam evaporation of CZTSe compound synthesized by solid state reaction method is investigated from XRD characterization to get a view about the structural parameters. Figure 2 represents the typical XRD pattern of CZTSe sample 1 and reveals the formation of some phases like Se,  $\text{Sn}_{0.9816}\text{Se}$ , Sn, Cu, Zn and CZTSe. Most intense peak belonging to  $2\theta$  value at  $38.79^\circ$  corresponds to CZTSe phase

with hkl parameters of (114) with d-spacing of 2.319 Å.[2] Another intense peak found at 23.56° belongs to Se with d-spacing of 3.7736Å.[4] Structural parameters are tabulated in the table 3 below.

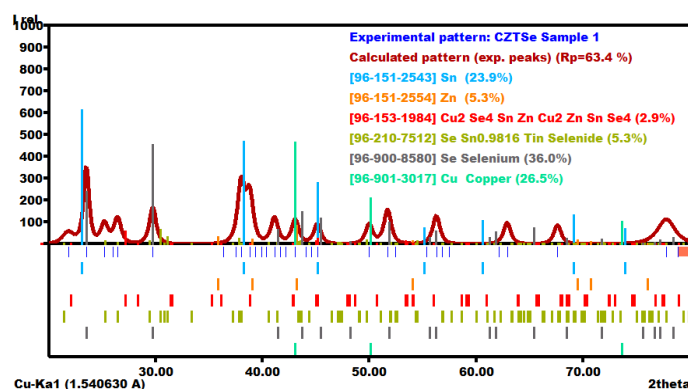


Fig. 2. XRD pattern of CZTSe Sample 1.

Table 3. CZTSe thin film formed by solid state reacted compound Sample 1.

Empirical formula	Crystal system	Space group	Unit Cell dimension (Å)		I/I <sub>c</sub>	c/2a	Density (calculated) gm/cm <sup>3</sup>	Wyckoff positions			
								X	Y	Z	
Se	Trigonal (hexagonal axes)	P 32 2 1 (154)	a= 4.35517	c= 4.94945	8.670 000	0.5682	4.83800	Se	0.127	0.00	0.167
Cu	cubic	F m -3 m (225)	a= 3.63600		11.99 0000	0.5	5.34800	Cu	0.00	0.00	0.000
Sn	Cubic	F d -3 m (227)	a= 6.65596		17.58 00	0.5	6.12700	Sn	0.00	0.00	0.00
Sn <sub>0.9816</sub> Se	Orthorhombic	P n m a (62)	a= 11.49417	b= 4.15096	8.080 000	0.1932	7.07300	Sn	0.118	0.250	0.103
			c= 4.44175					Se	0.855	0.250	0.482
Zn	Hexagonal	P 63/m m c (194)	a= 2.66169	c= 5.00397	10.90 0	0.9399	5.67600	Zn	0.33	0.667	0.750
Cu <sub>2</sub> ZnSnSe <sub>4</sub>	Tetragonal	I -4 2 m (121)	a= 5.68820	c= 11.33780	13.17 0000	0.9966	0.9959	Cu	0.000	0.50	0.250
								Zn	0.00	0.00	0.00
								Sn	0.00	0.00	0.50
								Se	0.259	0.259	0.371

It can be inferred from the spectra that a very little amount of CZTSe (2.9%) was formed in thin films formed by E-beam evaporation of bulk CZTSe compound. Major amount of Se is found and it could be related to the fact that melting point of Se is lowest among all elemental precursors.

Another peak is found denoting the  $\text{Sn}_{0.9816}\text{Se}$  phase at  $26.45^\circ$  and  $67.62^\circ$  belonging to hkl value of (210) and (113) respectively with orthorhombic crystal structure.[3] Cu in cubic structure belongs to  $Fm\bar{3}m$  (225) with  $I/I_c$  value of 11.99.[5]

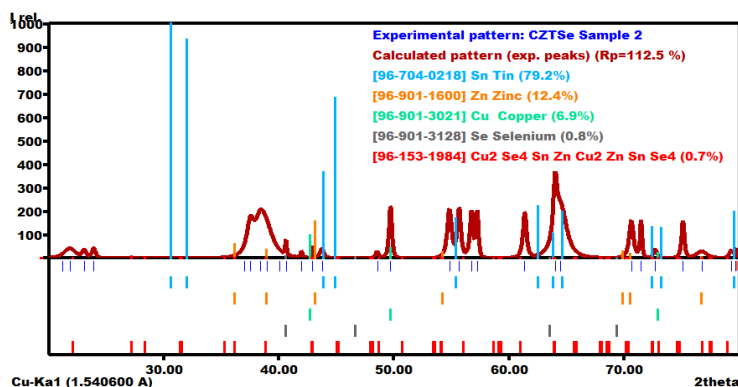


Fig. 3. XRD pattern for CZTSe Sample 2.

Parameters delineated from the study of XRD pattern of CZTSe sample 2 are presented in Table 4. There is clear evidence of the formation of CZTSe as a peak located at  $63.96^\circ$  with hkl value of (305) belongs to CZTSe phase.[14] Some secondary phases other than CZTSe is also observed in this sample like Se, Cu, Zn and Sn.[17-20].

Table 4. CZTSe thin film formed by solid state reacted compound Sample 2.

Empirical formula	Crystal system	Space group	Unit Cell dimension (Å)	$I/I_c$	c/2a	Density (calculated) $\text{gm/cm}^3$	Wyckoff positions			
							X	Y	Z	
Sn	Tetragonal	I 41/a m d (141)	a= 5.83230 c= 3.18230	11.460	0.2728	7.28400	Sn	0.00	0.250	0.875
Zn	Hexagonal	P 63/m m c (194)	a= 2.67000 c= 4.96600	10.9600	0.9288	7.08300	Zn	0.33	0.6250	0.250
Cu	Cubic	F m $\bar{3}$ m (225)	a= 3.66700	12.030000	0.5	8.56000	Cu	0.00	0.00	0.00
Se	Trigonal (hexagonal axes)	R $\bar{3}$ m (166)	a= 3.89200 c= 2.95720	10.70	0.3799	10.14000	Se	0.00	0.00	0.000
$\text{Cu}_2\text{ZnSnSe}_4$	Tetragonal	I $\bar{4}$ 2 m (121)	a= 5.68820 c= 11.33780	13.170000	0.9966	5.67600	Cu	0.00	0.50	0.250
							Zn	0.00	0.00	0.000
							Sn	0.00	0.00	0.50
							Se	0.259	0.259	0.371

Some amount of elemental precursors could be seen as the melting point of these precursors are different from each other so it could be related from the fact that each precursor was evaporated as they achieved their melting point during the deposition process. Peak at  $2\theta$  value of  $40.61^\circ$  and  $49.60^\circ$  belongs to Se and Cu elemental precursors respectively.

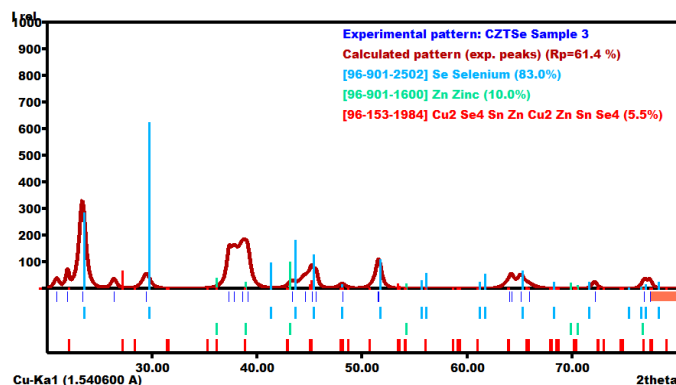


Fig. 4. XRD pattern of CZTSe sample 3.

XRD pattern of CZTSe sample 3 thin films reveals that this sample exhibited the three different phases like Zn, Se and CZTSe. CZTSe is belonging to space group of I-4 2 m (121).[2] Major amount of Se is detected in the sample 3.[21] It could be easily seen from analysis of compositional aspects that CZTSe is formed in very little quantity from bulk CZTSe compound in thin films. Highest amount of Se is detected in this sample.

Table 5. CZTSe thin film formed by solid state reacted compound Sample 3.

Empirical formula	Crystal system	Space group	Unit Cell dimension (Å)	I/I <sub>c</sub>	c/2a	Density (calculated) gm/cm <sup>3</sup>	Wyckoff positions			
							X	Y	Z	
Cu <sub>2</sub> ZnSnSe <sub>4</sub>	Tetragonal	I-4 2 m (121)	a= 5.68820 c= 11.33780	13.17 0000	0.9966	5.67600	Cu	0.00	0.50	0.250
							Zn	0.00	0.00	0.00
							Sn	0.00	0.00	0.50
							Se	0.259	0.259	0.371
Zn	Hexagonal	P 63/m m c (194)	a= 2.67000 c= 4.96600	10.960 000	0.9299	7.08300	Zn	0.33	0.667	0.250
Se	Trigonal (hexagonal axes)	P 31 2 1 (152)	a= 4.36620 Å c= 4.95360	13.17 0000	0.56726	4.81000	Se	0.225	0.00	0.333

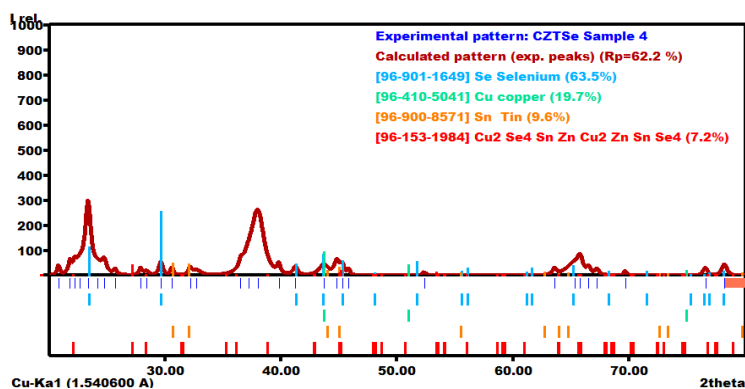


Fig. 5. XRD pattern of CZTSe sample 4 thin films.

Table 4. CZTSe thin film formed by solid state reacted compound Sample 4.

Empirical formula	Crystal system	Space Group	Unit Cell dimension (Å)	I/I <sub>c</sub>	c/2a	Density (calculated) gm/cm <sup>3</sup>	Wyckoff positions			
							X	Y	Z	
Se	Trigonal (hexagonal axes)	P 31 2 1 (152)	a= 4.36800 Å c= 4.95800	9.150 000	0.5675	4.80100	Se	0.225	0.00	0.33
Cu	Cubic	F m -3 m (225)	a= 3.58191	10.640 000	0.5	9.18400	Cu	0.00	0.00	0.000
Sn	Tetragonal	I 41/a m d (141)	a= 5.81970 c= 3.17488	11.46 0000	0.2727	7.33300	Sn	0.00	0.00	0.00
Cu <sub>2</sub> ZnSnSe <sub>4</sub>	Tetragonal	I -4 2 m (121)	a= 5.68820 c= 11.33780	13.17 0000	0.9966	5.67600	Cu	0.000	0.50	0.250
							Zn	0.00	0.00	0.00
							Sn	0.00	0.00	0.50
							Se	0.259	0.259	0.371

Thin films synthesized from solid state reacted compound sample 4 were composed of phases like Se, Sn, Cu and CZTSe from study of XRD pattern. Major peak belongs to CZTSe phase at  $2\theta$  value of  $65.81^\circ$  with hkl value of (008). Another peaks found at  $2\theta$  value of  $23.43^\circ$ ,  $30.64^\circ$  and  $43.71^\circ$  are relating to Se, Sn and Cu with d-spacing of  $3.7936\text{Å}$ ,  $2.9157\text{Å}$  and  $2.0693\text{Å}$  respectively.[16,22,23]

XRD result analysis of Sample 5 confirms that it exhibited the phase of Cu, Sn, Se and Cu<sub>2</sub>ZnSnSe<sub>4</sub>. Most intense peak at  $38.74^\circ$  belongs to Cu<sub>2</sub>ZnSnSe<sub>4</sub> phase.[2] Peak located at the  $2\theta$  value of  $23.55^\circ$ ,  $64.74^\circ$  and  $49.68^\circ$  attribute the phase of Se, Sn and Cu with d- spacing of  $3.7745\text{Å}$ ,  $1.4387\text{Å}$  and  $1.8337\text{Å}$  respectively.[16,17] Figure 6 represents the XRD spectra of CZTSe sample 5. An increment in the quantity of CZTSe is seen in this thin film as it increased upto 18.7%.

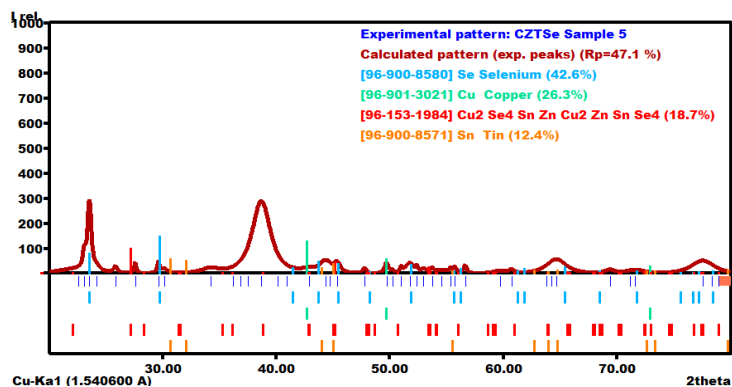


Fig. 6. XRD pattern of CZTSe Sample 5.

Table 7. CZTSe thin film formed by solid state reacted compound Sample 5.

Empirical formula	Crystal system	Space group	Unit Cell dimension (Å)	I/I <sub>c</sub>	c/2a	Density (calculated) gm/cm <sup>3</sup>	Wyckoff positions			
							X	Y	Z	
Se	Trigonal (hexagonal axes)	P 32 2 1 (154)	a= 4.35517 c= 4.94945	8.670	0.5682	4.83800	Se	0.217	0.00	0.167
Cu	Cubic	F m -3 m (225)	a= 3.66700	12.03 0000	0.5	8.56000	Cu	0.00	0.00	0.00
Cu <sub>2</sub> ZnSnSe <sub>4</sub>	Tetragonal	I -4 2 m (121)	a= 5.68820 c= 11.33780	13.17 0000	0.9966	5.67600	Cu	0.00	0.50	0.250
							Zn	0.00	0.00	0.00
							Sn	0.000	0.00	0.500
							Se	0.259	0.259	0.371
Sn	Tetragonal	I 41/a m d (141)	a= 5.81970 c= 3.17488	11.46	0.2727	7.3330	Sn	0.00	0.00	0.00

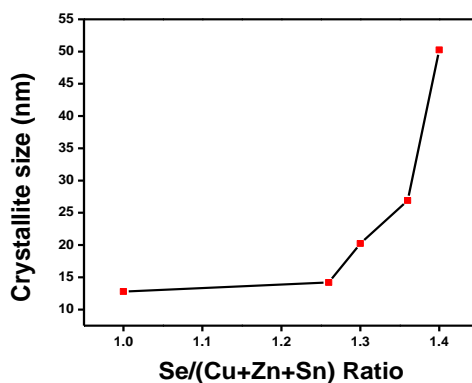


Fig. 7. Variation in crystallite size with respect to Se/(Cu+Zn+Sn) ratio.



Fig. 7 shows variation in crystallite size relative to  $\text{Se}/(\text{Cu}+\text{Zn}+\text{Sn})$  ratio. Crystallite size presented an increasing trend towards the increment in the value of  $\text{Se}/(\text{Cu}+\text{Zn}+\text{Sn})$  ratio.

### 3.3. SEM EDX result analysis

Fig. 8 shows the SEM images of CZTSe thin films from sample 1 to sample 5 with respect to compositional variation deposited on Soda Lime glass substrate. Formation of rod arrays connecting to each other at the center was observed in SEM images for the thin films of  $\text{Cu}_2\text{ZnSnSe}_4$  thin films. Sample 1 showed inter-particle distance and area of  $0.075 \mu\text{m}$  and  $0.006000 \mu\text{m}^2$  respectively. Inter-particle distance is found to be increased with respect to  $\text{Se}/(\text{Cu}+\text{Zn}+\text{Sn})$  ratio and its variation is tabulated in Table 8.

Table 8. Inter-particle distance variation in CZTSe thin films.

Sample	Inter particle distance ( $\mu\text{m}$ )	Area ( $\mu\text{m}^2$ )
1	0.075	0.0060
2	0.170	0.0175
3	0.250	0.0150
4	0.175	0.0175
5	0.275	0.0450

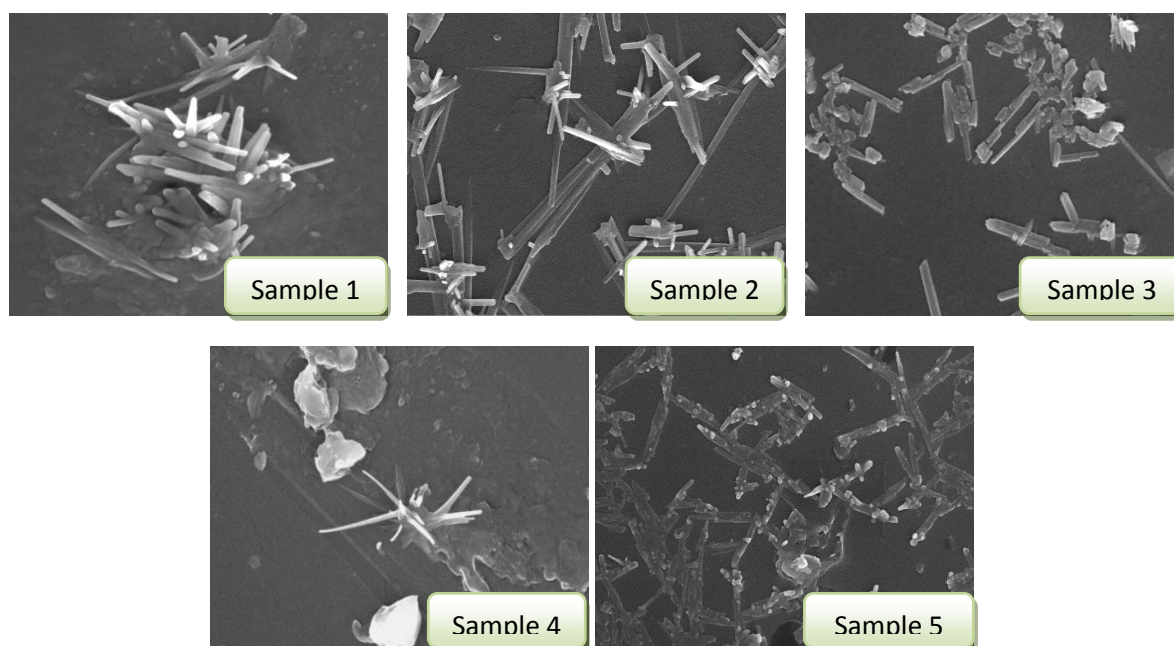


Fig.8. FESEM images of CZTSe samples

Various atomic ratios obtained from EDS results for CZTSe thin films grown with different sedimentary sequences, are shown in Table 9. FESEM mapping spectra of all CZTSe thin films is shown in figure 9. As expected, the elemental ratio of constituents during the deposition of thin films from bulk changes after deposition. The  $\text{Cu}/(\text{Zn}+\text{Sn})$  ratio for all CZTSe thin films ranges from 0.80-0.90. The content of Se is observed more in thin films which may be due to lowest melting point of Se amongst all constituents. Furthermore the ratio of  $\text{Cu}/\text{Sn}$  is found relatively unchanged for all samples. But it could be inferred from the analysis that all CZTSe thin films samples retained their stoichiometry almost nearly to stoichiometry of bulk CZTSe material.

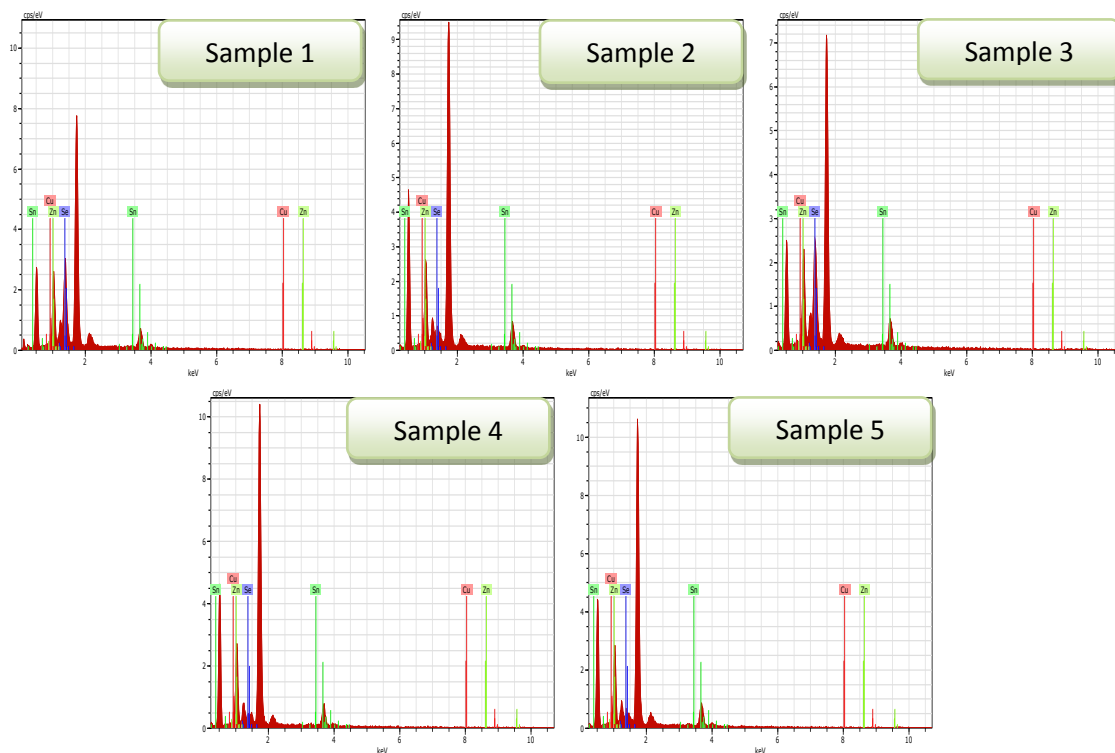


Fig. 9. FE-SEM mapping spectra recorded for CZTSe compound.

Table 9. The composition of the CZTSe thin films determined by EDX analysis.

Sample ID	Elemental composition at (%)			
	Cu/Zn	Cu/Sn	Se/(Cu+Zn+Sn)	Cu/(Zn+Sn)
Sample 1	1.90	1.94	0.98	0.80
Sample 2	1.88	1.95	1.32	0.89
Sample 3	1.95	1.94	1.26	0.87
Sample 4	1.74	1.75	1.30	0.85
Sample 5	1.65	1.98	1.20	0.90

#### 4. Conclusion

A study of CZTSe thin films fabricated from the pre-synthesized solid state reacted CZTSe compound using e- beam method shows that variation in Cu/(Zn+Sn) ratio highly affects the formation of secondary phases like  $\text{Sn}_{0.9816}\text{Se}$ , Se, Cu, Zn and Sn along with formation of CZTSe as single phase Se is found in almost samples (1-5) and it could be due to lowest melting point of Se in among all elemental constituents in CZTSe solid state reacted compound. An analysis of FESEM results of CZTSe thin films confirms that the stoichiometry retained during the deposition of CZTSe thin films and are almost matching with CZTSe solid state reacted compound. An increment in crystallite size is observed with the increment in Cu/(Zn+Sn) ratio.

## References

- [1] S. Kim, J. Kim, *Thin Solid Films* **547**, 178 (2013).
- [2] P.U. Bhaskar, G.S. Babu, Y.K. Kumar, V.S. Raja, *Solar Energy Materials and Solar Cells* **115**, 181 (2013).
- [3] G. Kaune, S. Hartnauer, F. Syrowatka, R. Scheer, *Solar Energy Materials and Solar Cells* **120**, 596 (2014).
- [4] W. Septina, S. Ikeda, T. Harada, M. Matsumura, *Physica Status Solidi C* **10**(7- 8), 1062 (2013).
- [5] M.I. Khalil, R. Bernasconi, L. Pedrazzetti, A. Lucotti, A. Le Donne, S. Binetti, L. Magagnin, *Journal of The Electrochemical Society* **164**(6), D302 (2017).
- [6] L. Shao, J. Zhang, C. Zou, W. Xie, *Physics Procedia* **32**, 640 (2012).
- [7] C. Sripan, R. Ganesan, R. Naik, A.K. Viswanath, *Optical Materials* **62**, 199 (2016).
- [8] F.I. Lai, J.F. Yang, Y.L. Wei, S.Y. Kuo, *Green Chemistry* **19**(3), 795 (2017).
- [9] M.V. Yakushev, I. Forbes, A.V. Mudryi, M. Grossberg, J. Krustok, N.S. Beattie, M. Moynihan, A. Rockett, R.W. Martin, *Thin Solid Films* **582**, 154 (2015).
- [10] M.A. Olgar, B.M. Başol, Y. Atasoy, M. Tomakin, G. Aygun, L. Ozyuzer, E. Bacaksız, *Thin Solid Films* **624**, 167 (2017).
- [11] I.D. Olekseyuk, O.V. Marchuk, I.V. Dydchak, L.D. Gulay, L.V. Piskach, O.V. Parasyuk, *Journal of Alloys Compd.* **340**, 141 (2002).
- [12] G.E. Delgado, A.J. Mora, G. Marcano, C. Rincon, *Materials Research Bulletin* **38**, 1949 (2003).
- [13] K. Lejaeghere, V. Van Speybroeck, G. Van Oost, S. Cottenier, *Critical Reviews in Solid State and Materials Sciences* **39**(1), 1 (2014).
- [14] I.D. Olekseyuk, O.V. Marchuk, I.V. Dydchak, L.D. Gulay, L.V. Piskach, O.V. Parasyuk, *Journal of Alloys Compd.* **340**, 141 (2002).
- [15] M. Sist, J. Zhang, B. Brummerstedt Iversen, *Acta Crystallographica Section B: Structural Science, Crystal Engineering and Materials* **72**(3), 310 (2016).
- [16] R. W. G. Wyckoff, Second edition. Interscience Publishers, New York, New York, *Crystal Structures* **1**, 7 (1963).
- [17] I.-K. Suh, H. Ohta, Y. Waseda, *Journal of Materials Science* **23**, 757 (1988).
- [18] M. C. Allison, M. Avdeev, S. Schmid, S. Liu, T. Söhnle, C. D. Ling, *Dalton transactions* **45**(23), 9689 (2016).
- [19] A. W. Hull, W. P. Davey, *Physical Review* **17**, 549 (1921).
- [20] Y. Akahama, M. Kobayashi, H. Kawamura, *Japanese Journal of Applied Physics* **31**, 1621 (1992).
- [21] P. Cherin, P. Unger, *Inorganic Chemistry* **6**, 1589 (1967).
- [22] R. Keller, W. B. Holzappel, H. Schulz, *Physical Review B* **16**, 4404 (1977).
- [23] A.D. Fortes, E. Suard, M.H. Lemée-Cailleau, C. J. Pickard, R.J. Needs, *Journal of the American Chemical Society* **131**(37), 13508 (2009).